Diffusion at Polymer/Polymer Interfaces Probed by Rheological Tools

M. Bousmina,*,† Hua Qiu,† M. Grmela,‡ and J. E. Klemberg-Sapieha§

Department of Chemical Engineering, CERSIM, Université Laval, Sainte-Foy, Québec (QC) G1K 7P4, Canada, and Departments of Chemical Engineering and of Engineering Physics, Ecole Polytechnique, Box 6079, Montréal (QC) H3C 3A7, Canada

Received April 13, 1998; Revised Manuscript Received August 31, 1998

ABSTRACT: Diffusion at the polymer/polymer interface was probed by small-amplitude oscillatory shear measurements carried out on polystyrene (PS)/polystyrene (PS) sandwich-like assembly as a function of the time of welding in the molten state. It was found that the dynamic complex shear modulus $G^*(t)$ at a fixed frequency increases with the time of contact in two time regimes. First $G^*(t)$ increases proportionally to $t^{1/2}$ and then a second regime takes place where $G^*(t)$ increases proportionally to $t^{1/4}$. At longer times, $G^*(t)$ tends asymptotically toward G^* of pure polystyrene. The results were interpreted in terms of reptation theory and the time of transition between the two scaling law regimes was found to be in agreement with the time needed for the transition from the Rouse mode to the reptation mode. Special attention was given to the initial state of the polymer surfaces before contact by performing experiments on (i) freshly prepared surfaces, (ii) presheared samples, (iii) fractured samples, and (iv) corona-treated samples. The results showed that the diffusion mechanism is strongly dependent on the initial chain-end distribution at the surface before contact. Diffusion at surfaces with an excess of chain ends proceeds in a Rouse-like mode, whereas for surfaces without excess of chain ends, the diffusion proceeds in a reptational-like dynamics, as was predicted by de Gennes and by Prager and Tirrell.

1. Introduction

When an assembly of two similar polymer surfaces is heated above the glass transition temperature, the macroscopic interface of the polymer/polymer sandwich-like assembly gradually disappears and the strength of adhesion increases as the voids in the contact area heal. Such a phenomenon has been attributed to the local interlacing of the neighboring chain ends in the contact region followed by a mass transfer of polymer chains across the interface. This type of diffusion process is encountered in many practical situations of polymer design and polymer processing whenever two polymer surfaces are brought into contact. This is the case for instance in film casting from a polymer dispersion where the dispersed particles diffuse and coalesce to form a continuous medium. Diffusion phenomena also occur in reactive polymer extrusion, blend compatibilization, and phase segregation and in injection molding at the weld line that appears in the contact area of the different moving fronts in the mold. Recently, diffusion has been becoming a challenging issue in medical and pharmaceutical applications such as controlled in situ or out situ drug delivery from polymeric gel or bioadhesion at the interface between a synthetic polymer and a biological substrate. This bioadhesion has been recently shown to be of paramount importance for promoting lesion repair and biological tissue regeneration.[1]

Polymer−polymer diffusion has to be distinguished from the two following cases: (i) diffusion of small molecules in a homogeneous medium formed by small molecules such as the diffusion of a solvent in another solvent or a colorant in a solvent and (ii) diffusion of small molecules (solvent for instance) in a polymer network of highly entangled chains. For the former, the mass transfer can be easily described by the classical Fick's law expressing the time evolution of the concentration profile by the following equation:

$$\frac{\partial C}{\partial t} = \nabla \cdot D \nabla C \tag{1}$$

where D is the diffusion coefficient, ∇ is the del operator, and C is the concentration.

For the latter, the diffusion mechanism becomes relatively complex; in the rubbery state, the diffusion mechanism is of Fickian type, whereas in the glassy state the time scale and the diffusion length scale cannot be predicted by the simple classical Fickian diffusional model. It is generally observed that at short times, a Fickian-like front moves as $\sqrt{t}$, and then an abrupt transition takes place where the dynamic diffusion mechanism is of a non-Fickian type.[2−6] The penetration of the solvent in the bulk polymer swells the chains network and thus introduces a supplementary stress that stretches the chains between entanglement junctions. This modifies the chains relaxation mechanism, which in turn modifies the diffusion process of the solvent. Such a behavior is known as case II diffusion and it is usually described by a modified form of Fick's law:[6]

$$\frac{\partial C}{\partial t} = \nabla \cdot [D(C) \nabla C + E(C) \nabla \sigma] \tag{2}$$

where the additional term $E(C)$ is the stress coefficient and σ is the stress induced by the penetration of the solvent that causes the swelling of the polymer network and the displacement of entanglement points. A systematic study of the coupling between the diffusion and the stresses in polymeric fluids is being recently studied in the context of the GENERIC method.[7−8]

The concept and the mechanism of diffusion become even more complicated when both the diffusing agent

* Corresponding author. E-mail: Bousmina@gch.ulaval.ca.
† Université Laval.
‡ Department of Chemical Engineering, Ecole Polytechnique.
§ Department of Engineering Physics, Ecole Polytechnique.

10.1021/ma980562r CCC: $15.00
Published on Web 10/30/1998

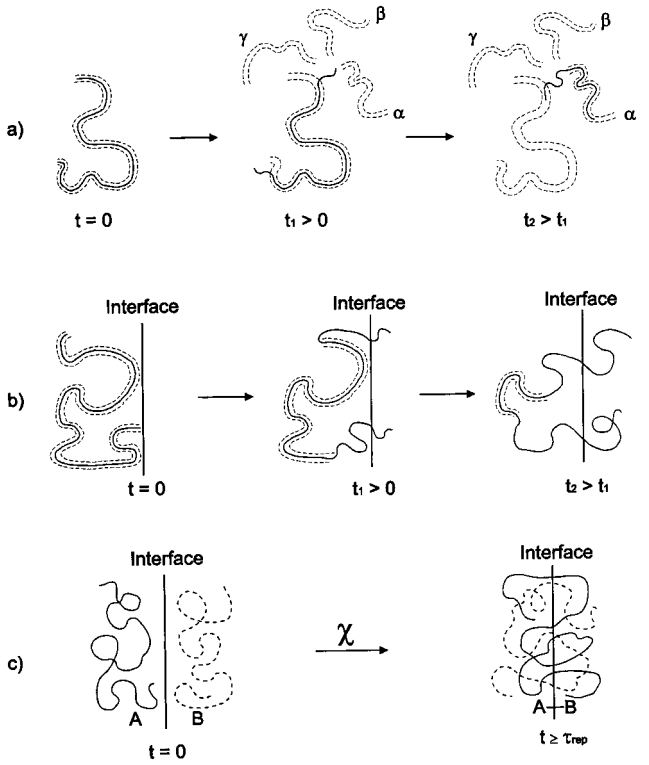

Figure 1. Reptation dynamics across a polymer/polymer interface.

and the medium of diffusion are highly entangled polymeric chains. In this case, more elaborate theories based on molecular dynamics are needed. The earliest molecular interpretation of the diffusion at polymer−polymer interfaces seems to be due to Voyutskii.[9] Subsequent experimental studies and modeling of the diffusion and the healing process at the polymer−polymer interfaces have been performed.[10−19] Experimental results of mechanical properties at the interface (fracture stress, fracture energy, fatigue crack propagation, deformation at rupture, etc.) have been interpreted in terms of the chain motion and modeled by the reptation model of de Gennes[20−24] (tube model). A schematic representation of reptational chain dynamics is illustrated in Figure 1a. In the reptation model, the movement of a single chain in a highly entangled medium such as a high molecular weight amorphous polymer is constrained by the presence of the entanglements of the neighboring chains, which act as local obstacles that cannot be crossed by the moving chain. The lateral displacements are thus excluded and the chain is seen as if it is confined in a conceptual fixed tubelike region having the same random-coil shape as the chain and representing the neighboring topological constraints. According to this molecular scheme, the single chain is forced to wriggle and to execute a random one-dimensional back-and-forth Brownian motion (reptation motion) during a certain time along the curvilinear length of the tube. At a certain moment, a portion of the chain slips out from the initial tube and enters, in a random manner, a new tube (α, β, or γ, ...) that is uncorrelated with the initial one (free random walk). At a longer time associated with the reptation time, τ_{rep}, the chain escapes completely from the initial tube and forgets totally its anterior configuration. This tube renewal by step reptational relaxations will continue till a dynamic equilibrium state is reached.

Doi and Edwards[25] rederived the tube model of de Gennes and found a general equation of the chain motion inside the tube that is quite similar to that previously found by de Gennes. The mean displacement is given by

$$\phi_n(t) = \langle (R_n(t) - R_n(0))^2 \rangle^{1/2} = \frac{1}{\sqrt{c}}\left[\frac{6k_BT}{N\zeta}t + \frac{4Nb^2}{\pi^2}\sum_{i=1}^{\infty}\frac{1}{i^2}\cos^2\left(\frac{i\pi n}{N}\right)(1 - \exp(-i^2 t/\tau_R))\right]^{1/2} \quad (3)$$

where c is a numerical parameter equal to 1 or 3 depending on the time scale, k_B is Boltzmann's constant, T is the absolute temperature, N is the number of monomers, b is the effective bond length, ζ is the friction coefficient, and t is the time. Different regimes (different scaling laws) can be readily deduced from eq 3 depending on the time scale and thus on the mechanism of chain dynamics inside the confining tube:

$$\phi_n(t) \approx \begin{cases} (t/\tau_R)^{1/4} & \text{for } t \le \tau_e \\ (t/\tau_R)^{1/8} & \text{for } \tau_e \le t \le \tau_R \\ (t/\tau_{rep})^{1/4} & \text{for } \tau_R \le t \le \tau_{rep} \\ (t/\tau_{rep})^{1/2} & \text{for } t \ge \tau_{rep} \end{cases} \quad (4)$$

These different regimes were also given by de Gennes.[26]

At very short times, $t < \tau_e$, the motion is restricted to the local Rouse segment. The chain does not feel the constraints of the network and behaves as a Rouse chain in a free space. The segmental motion propagates up to a length (at a time τ_e), e, comparable to the mesh size of the network, which can be reasonably approximated by the gyration radius, R_{ge}, of a chain with a molecular weight M_e, M_e being the molecular weight between entanglements:

$$R_{ge} = \left(\frac{C_\infty M_e j}{6M_0}\right)^{1/2} b_0 \quad (5)$$

where C_∞, M_o, j, and b_0 are the characteristic ratio ($\equiv b^2/b_0^2$), monomer molecular weight, number of backbone bonds per monomer, and bond length, respectively.

The Rouse relaxation time between entanglements, τ_e, is given by

$$\tau_e = \frac{e^4\zeta}{k_BTb^2} \quad (6)$$

For $\tau_e < t \le \tau_R$, the chain starts to feel the topological constraints of the tube and thus the motion of Rouse segments is restricted laterally but free motion is allowed along the curvilinear axis of the tube. However, the defects are not completely adjusted along the whole chain. When time τ_R is reached, the chain moves as a whole. The Rouse relaxation of the whole chain, τ_R, is given by

$$\tau_R = \frac{\zeta N^2 b^2}{3\pi^2 k_BT} \quad (7)$$

At $\tau_R < t < \tau_{rep}$, the defects are equilibrated along the total length of the tube and the chain moves as a whole along the fixed tube. The case of $t \ge \tau_{rep}$ is governed by a reptational process that allows the chain to completely

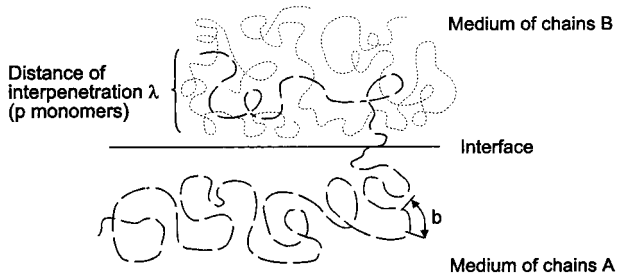

Figure 2. Interpenetration distance of p monomers of a chain A in the bulk of chains B.

escape from the initial tube. The memory of the initial conformation is then completely lost and the chain enters randomly in a new tube. The time τ_{rep} is given by

$$\tau_{rep} = \frac{\zeta N^3 b^4}{\pi^2 e^2 k_B T} \tag{8}$$

However, we should stress that the self-diffusion of a chain (or a monomer) in the bulk is different from the chain motion across an interface. The diffusion mechanism at the interface greatly depends on the configuration of the chain ends at the initial time of diffusion. Wool[16] discussed the diffusion across the interface in terms of the number of monomers $N(t)$ crossing the interface and found Fickian-type regimes $N(t) \approx t^{1/2}$ for $t \leq \tau_R$ and $t \geq \tau_{rep}$. For $\tau_R < t < \tau_{rep}$, Wool argued that the chain dynamics is governed by both Rouse and reptation motion. For negligible Rouse motion contribution, $N(t)$ becomes proportional to $t^{3/4}$.

To illustrate the diffusion process across an interface by reptational dynamics, let us consider a single chain placed near a given polymeric plane surface; due to the molecular dynamics illustrated by Figure 1a, the chain will be found at equilibrium at both sides of the surface (see Figure 1b). Now if two chains A and B with a given Flory interaction parameter (χ) are initially located at both sides of the interface, the degree and the length of interpenetration at equilibrium due to the reptational diffusion will depend on the degree of miscibility of the two chains represented by the χ parameter (Figure 1c).

de Gennes[27−29] and Prager and Tirrell[30] have described this diffusional process by simple (but not simplistic) molecular arguments. Let us briefly recall the molecular analysis of de Gennes. Consider a portion with p monomers ($p < N$, N being the total number of monomers) of a chain A diffusing across the interface in the region of chains B (Figure 2). To make their travel across the interface in the region B, the diffusing p monomers require a given energy:

$$U_p \approx \chi p k T \tag{9}$$

which is simply the Brownian energy of p monomers having the interaction parameter χ with the chains B. At equilibrium, the diffusion process stops and thus the energy is simply given by

$$U_p \approx kT \tag{10}$$

which implies that the number of monomers that have diffused in the region B scales as the inverse of the interaction parameter:

$$p \approx \chi^{-1} \tag{11}$$

The corresponding distance of penetration for $t < \tau_{rep}$ is given by

$$\lambda = bp^{1/2} \approx b\chi^{-1/2} \tag{12}$$

This means that for immiscible components (large χ), the interface is sharp, $\lambda < bN^{1/2} = R_0$, whereas for miscible or weakly immiscible components ($\chi \ll 1$), the interface is rather diffuse (interphase) and can be larger than R_0 for completely miscible components, R_0 being the statistical dimension of the random coil chain.

In the transient regime, the distance of penetration is a time-dependent function: $\lambda(t) \sim (t/\tau_{rep})^{\alpha}$. In the context of welding of polymer interfaces, a given macroscopic property (for instance the strength of the welded surfaces) can be thus reasonably assumed to be proportional to the density (or concentration) of the links across the interface which is itself proportional to the time of welding and thus proportional to the time of diffusion:

$$P(t) \sim \lambda(t) \sim (t/\tau_{rep})^{\alpha} \tag{13}$$

de Gennes[27−29] has distinguished several cases depending on the time scale and the magnitudes of $N_e\chi$ and $NN_e\chi^2$ (N_e is the number of monomers between entanglements) and on the initial configuration of the chain ends at the interface. We recall here only the two cases of interest.

(i) If the chain ends are initially concentrated at the polymer surface before contact, then the diffusion process proceeds in a Rouse-type dynamics, which means that the exponent and thus the macroscopic property scale in time as

$$P(t) \sim P_{bulk}(t/\tau_{rep})^{1/4} \tag{14}$$

(ii) In contrast, if the chain ends are not initially concentrated at the interface, but they have to first diffuse in the bulk before reaching the interface, the exponent in this case is $\alpha = 1/2$ and hence the macroscopic property P varies in time as

$$P(t) \sim P_{bulk}(t/\tau_{rep})^{1/2} \tag{15}$$

Earlier experiments on the healing of cracks at the fractured surfaces performed by Kausch and coworkers[10−13] showed effectively that refracture stress grows as $t^{1/4}$. This is the first case discussed by de Gennes[27−29] and by Prager and Tirrell,[30] where the initial fracture has generated an excess of chain ends at the initial surfaces before welding.

On the other hand, Wool et al.[14−18] performed several lap shear experiments on freshly molded samples and found that the fracture stress at the welded polymer interface increases with the healing time as

$$\sigma(t) \sim t^{1/4} \tag{16}$$

Wool et al. focused their analysis on the entanglements across the interface and argued that the above scaling law is valid whenever the chains in the deformation region disentangle completely.

The present work was undertaken to verify the feasibility of studying the diffusion at the polymer/polymer interface by rheological testing under both high and low deformation flows. In this first paper we report only the results obtained on the symmetric A/A polymer

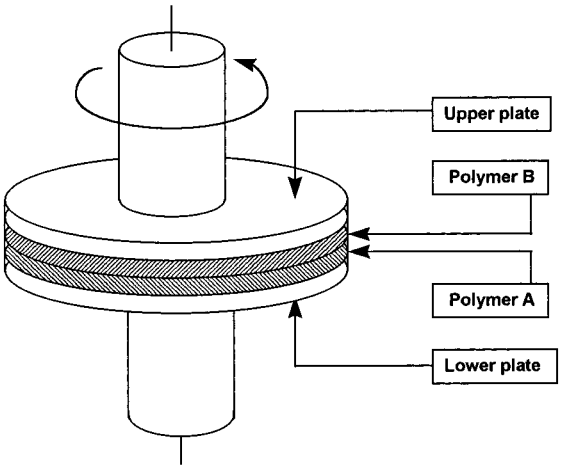

Figure 3. Sample setup for rheological testing.

assembly in the frame of linear viscoelasticity, where no modification of the structure and thus no disentanglement due to the external deformation field is presumed to occur. The purpose is to discuss the initial distribution of chain configurations at the interface with connection to diffusive and linear viscoelastic properties of sheared polymer/polymer surface assemblies. Different cases of initial polymer surfaces are examined: (i) diffusion on a polymer/polymer assembly of freshly molded and annealed samples, (ii) diffusion on a preshеared polymer/polymer assembly, (iii) diffusion on a polymer/polymer assembly of fractured samples, and (iv) diffusion on a polymer/polymer assembly of a previously corona-treated sample.

To our knowledge, this is the first time that diffusion at molten polymer/polymer surfaces is probed by rheological tools.[31]

2. Experimental Section

2.1. Materials. Polystyrene (PS) was obtained from Dow Chemical Inc. It has a weight-average molecular weight M_w = 375 600 and M_w/M_n = 1.27 (monodisperse PS are currently under study). The samples for rheological measurements were prepared by compression molding at 180 °C in the form of 25 mm diameter and 0.75 mm thick disks using well-cleaned and polished plates (mirror quality surfaces). The samples were then annealed at 85 °C under vacuum for 1 week to remove eventual surface contamination and to allow relaxation of oriented chains at the surface due to compression.

2.2. Sample Preparation and Viscoelastic Measurements. The measurements were carried out on a CVO−Bohlin constant stress rheometer in parallel plate geometry. The sample setup for rheological testing is depicted in Figure 3. Usually, only one disk is used between the two plates of the rheometer for rheological measurements. In this work a sandwich-like assembly of two or more PS/PS layers was placed between the two parallel plates[31] (increasing the number of PS thin layers of 0.1−0.3 mm thick in the sandwich increases the contribution of the interface; for clarity purposes this case will not be discussed here).

A rigorous procedure was followed to get clean specimens and to minimize experimental errors of sample preparation. In all experiments, gloves were worn to prevent surface contamination. The two PS disks of 0.75 mm in thickness each and with smooth surfaces were brought in contact at room temperature and were well aligned before placing them between the two parallel plates of the rheometer, which were previously heated and maintained at constant temperature T = 135 °C. Such manipulation has to be fast and carefully executed to avoid a rapid decrease of the plate temperature. The polymer sandwich was then slightly compressed to get a gap of 1.48 mm. The oscillatory shear measurements were then started after 10 min required for thermal equilibrium, as was verified by thin thermocouples placed at different points in the bulk of the sample (separate sample). To verify the effect of pressure, different gaps were tested and reproducible results were obtained. Also other sandwich samples were first annealed, without pressure, in the oven at 135 °C for different times before placing them between the parallel plates of the rheometer; this did not change the results. Nevertheless, the pressure is expected to affect the diffusion process and thus the interpenetration distance proportionally to e^{-P}; however, since the same dimensions of the samples and the same gap were used for all tests, the pressure effect should be quite similar from one experiment to the other and will not affect the relative comparative study of the polymer−polymer diffusion. All measurements were conducted at 135 °C under purge of dry nitrogen in the linear viscoelastic regime.

The complex shear modulus G^* of the PS/PS sandwich sample was measured as a function of frequency using the following shear deformation history. A first small-amplitude oscillatory shear was applied and then the sample was left at rest between the parallel plates of the rheometer at the same temperature for a given interval of time without shear, and then a second small-amplitude oscillatory shear was applied. This successive dynamic-and-static regimes were repeated several times to follow the evolution of $G^*(\omega)$ with time. Measurements of G^* were also carried out as a function of time at a fixed frequency (ω = 1 Hz).

2.3. Corona Treatment and XPS Analysis. Corona treatment was performed with a homemade device. A detailed description of this device is given elsewhere.[32] It consists of two flat aluminum electrodes separated by a quartz-dielectric plate. Several Teflon rings were mounted on one electrode to form a cylindrical cell with adjustable length. The treatment has been performed under conditions of 10 kV and 20 mA at 3.5 kHz for 60 s. The surface chemical structure of corona-treated PS disks has been determined by X-ray photoelectron spectroscopy (XPS) using a VG-ESCALAB 3 MkII surface analytical instrument. The Mg Kx achromatic X-ray source (1253.6 eV) was operated at 15 kV, with an emission current of 20 mA. The pressure inside the chamber of analysis was kept below 10^{-9} Torr during the measurements. The sample holder was oriented at 45° with respect to the analyzer. The collecting time of the spectra was 5 min for both the broad- (0−1000 eV) and the high-resolution scans. The inelastic background was subtracted using Shireley's method.[33] A curve-fitting SURFSOFT program has been used, which permits variation of the curve parameters such as the Gaussian/Lorentzian ratio, the full width at half-maximum (fwhm) and the peak positions. The quality of the curve fitting was evaluated by chi-square convergence. The surface composition of the corona-treated surface has been determined from the intensities of C1s and O1s in the broad scan XPS spectrum.

3. Results and Discussion

3.1. Diffusion on Freshly Molded Samples. Figure 4 shows the variation of (PS/PS) G^* as a function of frequency for different times of contact. G^* clearly increases as a function of the contact time. At short times, the increase is more evident at high than at low frequencies, and for long times the increase is observed over the whole frequency range. This suggests that in the first stage of diffusion, segregation phenomena take place due to the diffusion of chains with small relaxation times. Longer chains need more time to rearrange their conformation and to participate to the net mass transfer across the interface. The magnitude of G^* time evolution depends on the frequency window, but the local velocity of G^* increase (slope of $G^* = f(t)$) does not depend on the frequency in the region $\omega > \omega_c = 0.2$ rad/s. The magnitude of G^* is not spectacular, but the slope of the increase was found to be firmly reproducible. Reproducibility within 5% of error was confirmed on

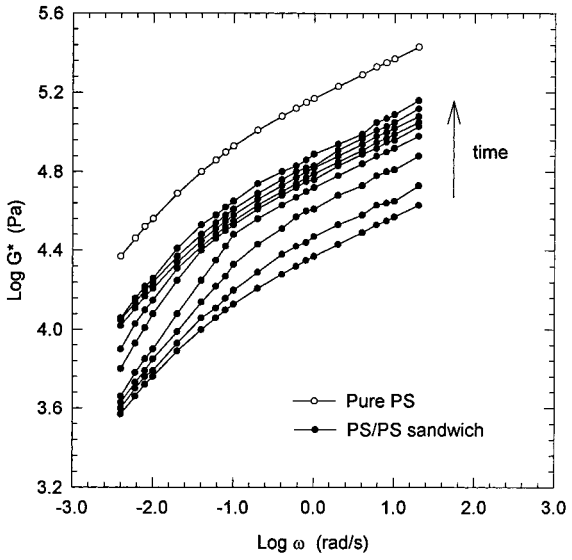

Figure 4. $G^*(\omega)$ variation of virgin PS/PS sandwich-like assembly for different times of welding.

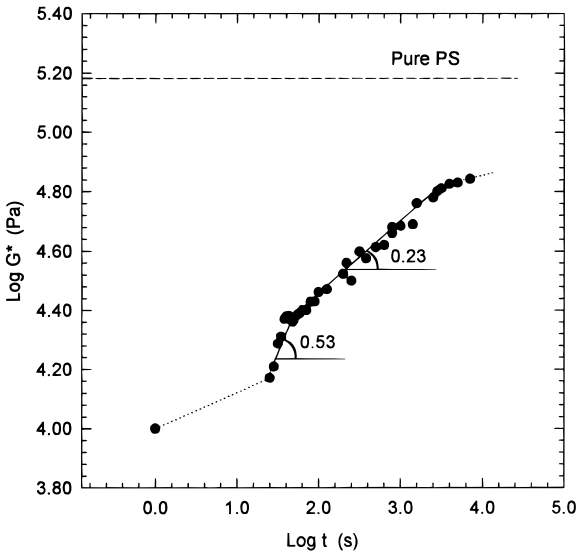

Figure 5. G^* variation of virgin PS/PS sandwich-like assembly as a function of time at $\omega = 1$ Hz.

more than five experiments conducted on similar samples under the same conditions.

G^* was then measured as a function of time at a fixed frequency ($\omega = 1$ Hz). A typical example of $G^*(t, \omega = 1$ Hz) evolution is shown in Figure 5. $G^*(t)$ increases linearly with time (in logarithmic scale) in two time regions and then tends, for long times, toward a plateau having a magnitude lower but asymptotically close to the G^* of pure PS. The straight line for the two first points was only drawn for better visualization. In log−log scale, $G^*(t)$ first increases with a slope of 0.53 and then a transition occurs at approximately $t_c = 59$ min and the slope of $G^*(t)$ becomes about 0.23. This behavior is not expected. Owing to the theory, G^* is proportional to $\phi_n(t)$, and thus the transitions in time should occur in the order predicted by eq 4; i.e., the slope of 1/4 should precede the slope 1/2. One can a priori presume that the obtained slopes are positioned in the inverse order. However, the calculation of the different relaxation times, $\tau_e = 22$ s; $\tau_R = 49.5$ min, and $\tau_{rep} = 6864$ min, shows that is not the case. In fact, τ_R is the only time that can be identified to the experimental relaxation time $t_c = 59$ min. The transition between the scaling laws $G^* \propto t^{1/2}$ and $G^* \propto t^{1/4}$ occurs at τ_R rather than at τ_{rep}.

The calculation of τ_e, τ_R, and τ_{rep} was obtained from the following numerical values: $M_0 = 104$, $b_0 = 1.54$ Å, $M_w = 375\,600$, $k_B = 1.380 \times 10^{-23}$ J/K, $T = 408$ K (135 °C), $\zeta = 1.6 \times 10^{-4}$ (N·s)/m)[34] and the parameter b can be calculated as a function of the characteristic ratio, C_∞, and the bond length, b_0, as $b = (C_\infty b_0^2)^{1/2}$ with ($C_\infty = 10$)[16] and $e \approx R_{ge} = 36.47$ Å, as calculated from eq 5 with $j = 2$. Substituting these values into eqs 6−8, we obtain $\tau_e = 22.5$ s, $\tau_R = 49.5$ min, and $\tau_{rep} = 6863.8$ min.

The unexpected behavior observed in Figure 5 might therefore be argued by the following molecular dynamics: the two polymer disks were obtained by compression molding, so before bringing them into contact the chain ends were concentrated in the bulk rather than at the surface. Some chains were perhaps oriented in the plan of compression (see Experimental Section: annealing of the compressed samples was carried out to minimize the effect of the chains orientation at the surface), but there is no reason the chain ends should be initially concentrated at the surface, which is a thermodynamically unfavorable configuration. Thus the chain ends first diffuse in the bulk before reaching the interface and traveling into the first layer of the other region. Some chains, mainly the small ones have effectively crossed the interface and penetrated the bulk of the other side of the sandwich. However, due to their slow motion, long chains reach the interface and adopt for a given period of time a pseudoequilibrium configuration. This first stage of diffusion is characterized by an exponent close to 1/2 of the scaling law, as was discussed by de Gennes. Then the second diffusion process takes place with an initial state (the end of the first stage) characterized by an excess of chain ends at the interface, which promotes the chains of one side to penetrate the bulk of the other side of the interface with an exponent close to 1/4 of the scaling law of diffusion.

To better clarify the effect of the initial chain ends distribution at the polymer surfaces before contact, three types of additional experiments were carried out (i) diffusion on pre-sheared samples, (ii) diffusion on fractured samples, and (iii) diffusion on corona-treated samples.

3.2. Diffusion on Preshear Samples. The PS/PS sandwich was placed between the two parallel plates of the rheometer and the dynamic modulus G^* was first measured as a function of frequency under small-amplitude oscillatory shear. The dynamic regime was then stopped and the sample was immediately submitted to a steady shear flow at shear rate $\dot{\gamma} = 2$ s^{-1} for 20 s, that is a deformation of 40%. Then a time sweep experiment at $G^*(t, \omega = 1$ Hz) was carried out. The obtained results are reported in Figure 6. The G^* after steady shear lies below G^* of the initial sample (reproducible results), and then G^* increases again linearly on a log−log plot with the contact time.

Without preshear and within the first 60 min (time of transition 59 min), we should observe, as was found in the previous section, an increase of $G^*(t)$ with an exponent 1/2 on the log−log scale. The results show instead an exponent of 0.32 (between 1/4 and 1/2). This suggests that the pre-shear has perturbed the chains configuration at the interface and perhaps has extracted some chains that have diffused in the other side of the interface. Thus, the small-amplitude dynamic tests

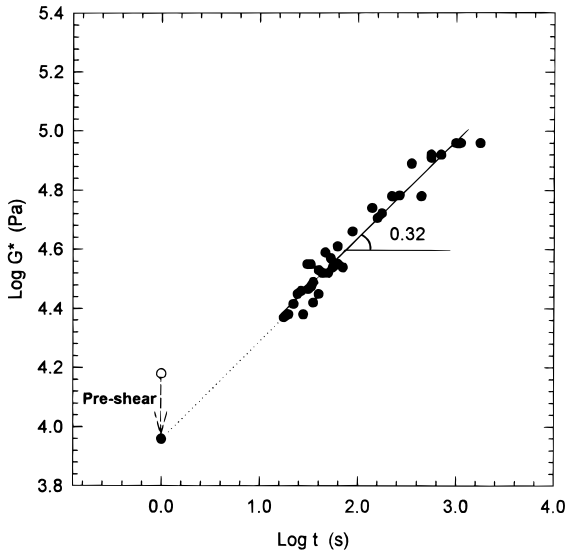

Figure 6. G^* variation of a presheared PS/PS sample as a function of time at $\omega = 1$ Hz.

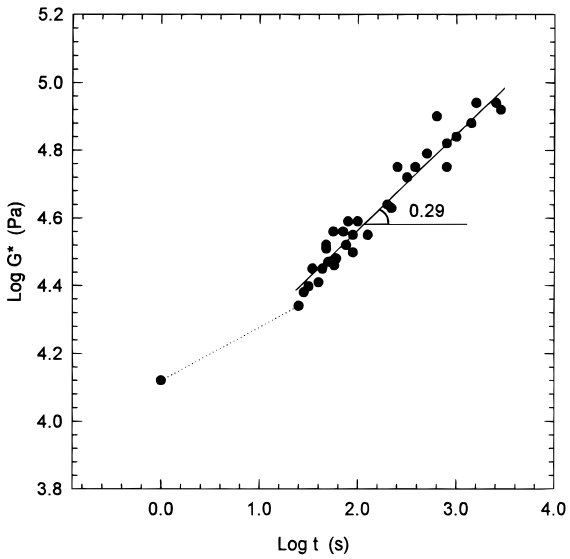

Figure 7. G^* variation of a fractured PS/PS sandwich-like assembly as a function of time at $\omega = 1$ Hz.

performed after the preshear take place with an initial state characterized by a certain excess of the chain ends at the interface. However, the concentration of chain ends resulting from the preshear is not enough to allow discrimination between the two scaling laws.

3.3. Healing of Fractured Samples. To start with an initial state characterized by a high concentration of chain-ends, a sample of 25 mm in diameter and 1.4 mm in thickness was molded as described in the Experimental Section and then fractured in the median region of thickness. The two-half pieces were then immediately brought in contact and placed between the two parallel plates of the rheometer at 135 °C. The complex dynamic modulus $G^*(\omega = 1$ Hz) was then measured as a function of time. The typical time evolution of $G^*(t, \omega = 1$ Hz) is shown in Figure 7. The results show that $G^*(t)$ increases linearly with the time of healing with a slope of 0.29 that is close to the theoretical value (1/4) predicted by de Gennes[27−29] and by Prager and Tirrell.[30] This shows that diffusion at polymer/polymer interfaces is strongly dependent upon the initial configuration of chain ends before the welding

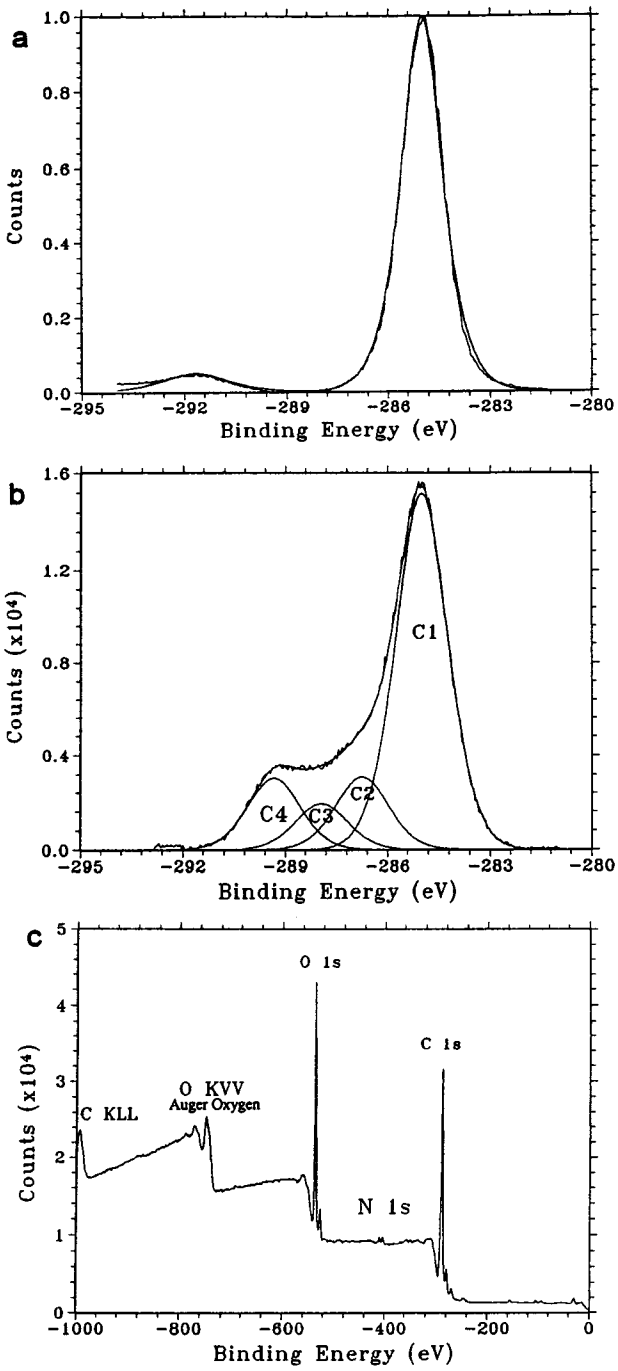

Figure 8. XPS spectra of an (a) untreated PS surface and (b) a corona-treated PS surface and (c) a broad scan of the PS corona-treated surface.

and confirms that the dynamic process discussed by de Gennes and by Prager and Tirrell occurs even in molten state.

Additional experiments of diffusion with a particular initial state of the polymer surface were conducted using surface treatment (corona treatment) of the two pieces of the sandwich before contact.

3.4. Diffusion on Corona-Treated Samples. The objective here is to artificially introduce some reactive groups on the surface of the PS disks before performing the welding. The two PS disks were treated by corona discharges as described in the Experimental Section. The effect of corona treatment on the surface composition is shown in Figure 8. A 23 wt % amount of oxygen was incorporated on the PS surface. The C1s for

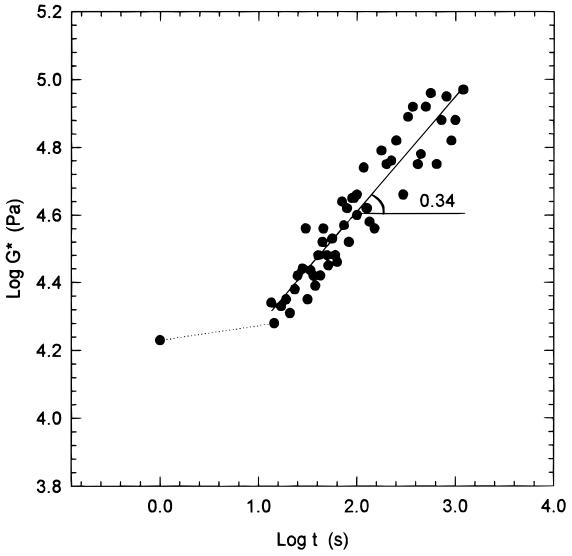

Figure 9. G^* variation of corona-treated PS/PS sandwich-like assembly as a function of time at $\omega = 1$ Hz.

untreated PS is composed of C1 at 285 eV, assigned to the C—C and C—H in the benzene ring. The aromatic cycle gives rise to a low intensity shakeup satellite peak C5 at 291.6 eV. Corona treatment clearly resulted in surface oxidation mainly of peak C2 associated with C—O (ether or hydroxyl at 286.5 eV) and peak C3 corresponding to carbonyl or double ether at 288.0 eV and peak C4 representing O═C—OH carbonyl or O═C—O—C ester groups at 289.4 eV. The broad scan spectrum also shows that nitrogen was introduced on the surface of PS by corona treatment.

These reactive groups are expected to affect the initial stage of diffusion when the two treated surfaces are brought into contact. Effectively, as shown in Figure 9, the slope of $G^*(t, \omega = 1$ Hz) is 0.34, which is closer to 1/4 than to 1/2. This suggests that the reactive species introduced by corona treatment act, via their local interactions, as a "locomotive" that promotes diffusion across the interface. However, since the reactive groups are not necessarily fixed on end groups, the diffusion mechanism is not exactly the same but it is close to the case of diffusion starting with an excess of chain ends at the initial surfaces. Additionally, corona treatment may have broken some chains and thus enlarged the molecular weight distribution, but this was not verified in this work (no GPC measurements were carried out on corona-treated samples).

We should also point out that, despite the reproducible data, the linear variations shown in Figures 6, 7, and 9 exhibit very similar exponents within experimental errors. The results reported are also expected to depend on molecular weight polydispersity that was ignored in this first paper. Samples with narrow and polydisperse molecular weights are currently studied in our laboratory.

4. Conclusions

The relationship between linear viscoelastic properties in the molten state and diffusion at polymer/polymer interfaces has been clearly demonstrated. The results revealed that the diffusion mechanism is strongly dependent on the initial configurational distribution of the chain ends at the surfaces before establishing the contact. For freshly molded samples, $G^*(t, \omega = 1$ Hz) of the sandwich-like assembly was found to increase in two time regimes identified by two scaling laws: $G^*(t) \cong t^{1/2}$ and then $G^*(t) \cong t^{1/4}$.

The results were interpreted in terms of reptation theory, and the time of transition between the two scaling law regimes was found to be in agreement with the time needed for the transition from the Rouse mode to the reptation mode. Additional experiments carried out on (i) presheared samples, (ii) fractured samples, and (iii) corona-treated samples revealed that the diffusion mechanism is strongly dependent on the initial chain ends distribution at the surface before contact. Surfaces with an excess of chain ends diffuse in a Rouse-like mode, whereas surfaces without an excess of chain ends diffuse in a reptational-like dynamics as was predicted by de Gennes[27−29] and by Prager and Tirrell.[30]

To the best of our knowledge it is shown for the first time in this paper that diffusion at molten polymer/polymer interfaces can be effectively probed by rheological tools. Our near future work is to examine the effect of polydispersity, surface/surface interactions through copolymer compatibilization, and chemical inter-reaction and establish a theoretical framework allowing determination of self-diffusion and mutual diffusion coefficients by using this novel technique.

Acknowledgment. We would like to gratefully thank Sir Professor Pierre Gilles de Gennes for attracting our attention on the role of the initial chain-end distribution before contact that we had completely ignored in the beginning of this work. This work was supported by the NSERC (Natural Sciences and Engineering Research Council of Canada) and the FCAR (Fonds pour la Formation de Chercheurs et l'Aide à la Recherche du Québec).

References and Notes

(1) Woerly, S.; Pinet, E.; de Robertis, L.; Bousmina, M.; Laroche, G.; Roitbak. *J. Biomater. Sci. Polym. Ed.* **1998**, *9*, 681.
(2) Edwards, D. A.; Cohen, D. S. *AIChE J.* **1995**, *41*, 2345.
(3) Hui, C. Y.; Wu, K. C. *J. Appl. Phys.* **1987**, *61*, 5137.
(4) Witelski, T. P. *J. Polym. Sci., Polym. Phys.* **1996**, *34*, 141.
(5) Edwards, D. A. *SIAM J. Appl. Math.* **1995**, *55*, 1039.
(6) Edwards, D. A. *J. Polym. Sci., Polym. Phys.* **1996**, *34*, 981.
(7) Grmela, M.; Öttinger, H. C. *Phys. Rev. E.* **1997**, *56*, 6620.
(8) Öttinger, H. C. *Phys. Rev. E.* **1997**, *56*, 6633.
(9) Voyutskii, S. S. *J. Adhesion* **1971**, *3*, 69.
(10) Jud, K.; Kausch, H. H.; Williams, J. G. *J. Mater. Sci.* **1981**, *16*, 204.
(11) Jud, K.; Kausch, H. H. *Polym. Bull.* **1979**, *1*, 697.
(12) Kausch, H. H. *Polymer Fracture*; Springer-Verlag: Berlin, New York, 1979, 252.
(13) Kausch, H. H.; Jud, K. Proceedings of the IUPAC, 26th International Symposium on Macromolecules, Mainz, 1979; p 17.
(14) Whitlow, S.; Wool, R. P. *Macromolecules* **1989**, *22*, 2648.
(15) Whitlow, S.; Wool, R. P. *Macromolecules* **1991**, *24*, 5926.
(16) See: Wool, R. P. *Polymer Interfaces: Structure and Strength*; Hanser Publications: Cincinnati, 1995.
(17) Kim, Y. H.; Wool, R. P. *Macromolecules* **1983**, *16*, 1115.
(18) Wool, R. P.; Yuan, B. L.; McGarel, O. J. *Polym. Eng. Sci.* **1989**, *29*, 1340.
(19) Wool, R. P.; O'Connor, K. M. *J. Appl. Phys.* **1981**, *52*, 5953.
(20) de Gennes, P. G. *J. Chem. Phys.* **1971**, *55*, 572.
(21) de Gennes, P. G. *Scaling Concepts in Polymer Physics*; Cornell University Press: Ithaca, New York 1979.
(22) de Gennes, P. G. *Hebd. Seances Acad. Sci., Ser. B* **1980**, *291*, 219.
(23) de Gennes, P. G. *Macromolecules* **1976**, *9*, 587.
(24) Daoud, M.; de Gennes, P. G. *J. Polym. Sci., Polym. Phys. Ed.* **1979**, *17*, 1971.
(25) Doi, M.; Edwards, S. F. *The Theory of Polymer Dynamics*; Clarendon Press: Oxford, U.K., 1986.
(26) de Gennes, P. G. *J. Chem. Phys.* **1980**, *72*, 4756.
(27) de Gennes, P. G. *C. R. Acad. Sci Paris, Sér. II* **1988**, 1841.

(28) de Gennes, P. G. *C. R. Acad. Sci Paris, t. 291, Série B* **1980**, 219.
(29) de Gennes P. G. In *Physics of Polymer Surfaces and Interfaces*; Sanchez I. C., Fitzpatrick, L. E., Eds.; Butterworth-Heinemann; Manning Publications Co.: London, 1992; p 55.
(30) Prager, S.; Tirrell, M. *J. Chem. Phys.* **1981**, *75*, 5194.
(31) Qiu, H.; Bousmina, M. XIIth International Congress on Rheology, August 18-23, 1996, Quebec City (Quebec), Canada.
(32) Klemberg-Sapieha, J. E.; Martinu, L.; Sapieha, S.; Wertheimer, M. R. In *The Interactions in Polymeric Composites*; Akovali, G., Ed.; Kluwer Academic Publishers: 1993; p 201.
(33) Shireley, D. A. *Phys. Rev.* **1972**, *B5*, 4709.
(34) Agrawal, G.; Wool, R. P.; Dozier, W. D.; Felcher, G. P.; Russell, T. P.; Mays, J. W. *Macromolecules* **1994**, *27*, 4407.

MA980562R